NUREG/CR-1026
PNL-3114
RE

Modified Finite Element Transport Model, FETRA, for Sediment and Radionuclide Migration in Open Coastal Waters

Y. Onishi
E. M. Arnold
D. W. Mayer

August 1979

Prepared for
the U.S. Nuclear Regulatory Commission

Pacific Northwest Laboratory
Operated for the U.S. Department of Energy
by Battelle Memorial Institute

Battelle

PNL-3114

PACIFIC NORTHWEST LABORATORY
operated by
BATTELLE
for the
UNITED STATES DEPARTMENT OF ENERGY
Under Contract EY-76-C-06-1830

Printed in the United States of America
Available from
National Technical Information Service
United States Department of Commerce
5285 Port Royal Road
Springfield, Virginia 22151

Price: Printed Copy $____*; Microfiche $3.00

*Pages	NTIS Selling Price
001-025	$4.00
026-050	$4.50
051-075	$5.25
076-100	$6.00
101-125	$6.50
126-150	$7.25
151-175	$8.00
176-200	$9.00
201-225	$9.25
226-250	$9.50
251-275	$10.75
276-300	$11.00

NUREG/CR-1026
PNL-3114
RE

MODIFIED FINITE ELEMENT TRANSPORT MODEL, FETRA, FOR SEDIMENT AND RADIONUCLIDE MIGRATION IN OPEN COASTAL WATERS

Y. Onishi
E. M. Arnold
D. W. Mayer

August 1979

Prepared for
the Division of Safeguards, Fuel Cycle, and Environmental Research,
U.S. Nuclear Regulatory Commission,
Under a Related Services Agreement with the
U.S. Department of Energy, Contract EY-76-C-06-1830
FIN No. B2271-9

Project: Mathematical Simulation of Sediment and Contaminant Transport in Surface Waters

Task: Transport of Sediment and Radionuclides in Oceans

Pacific Northwest Laboratory
Richland, Washington 99352

ABSTRACT

The finite element model, FETRA, simulates transport of sediment and radionuclides (and other contaminants, such as heavy metals, pesticides, and other toxic substances) in surface water bodies. The model is an unsteady, two-dimensional (longitudinal and lateral) model which consists of the following three submodels coupled to include sediment-contaminant interactions: 1) sediment transport submodel, 2) dissolved contaminant transport submodel, and 3) particulate contaminant (contaminant adsorbed by sediment) transport submodel.

Under the current phase of the study, FETRA was modified to include sediment-wave interaction in order to extend the applicability of the model to coastal zones and large lakes (e.g., the Great Lakes) where wave actions can be one of the dominant mechanisms to transport sediment and toxic contaminant. FETRA was further modified to handle both linear and quadratic approximations to velocity and depth distributions in order to be compatible with various finite element hydrodynamic models (e.g., RMA II and CAFE) which supply hydrodynamic input data to FETRA.

The next step is to apply FETRA to coastal zones to simulate transport of sediment and radionuclides with their interactions in order to test and verify the model under marine and large lacustrine environments.

EXECUTIVE SUMMARY

The modified finite element transport model, FETRA is capable of simulating transport of sediment and radionuclides (and other toxic contaminants) in coastal zones, large lakes (e.g., the Great Lakes), estuaries and rivers. However, since FETRA is a depth-averaged, two-dimensional model, its applicability to estuaries is limited to vertically well-mixed estuaries.

FETRA consists of the three submodels performing the following: The sediment transport submodel simulates transport, deposition and scouring of three sediment size fractions of cohesive and noncohesive sediments. These sediments can either be organic or inorganic. The submodel includes mechanisms of:

1. convection and diffusion/dispersion of sediments
2. wave motion to suspend and transport sediments
3. fall velocity and cohesiveness
4. deposition on the ocean and river bed
5. resuspension from the ocean and river bed (bed erosion and armoring)
6. sediment contributions from outside point and nonpoint sources

The dissolved and particulate contaminant transport submodels include mechanisms of

1. convection and diffusion/dispersion of dissolved and particulate contaminants
2. adsorption (uptake) of dissolved contaminants by sediments or desorption from sediments into water
3. radionuclide decay or other chemical and biological degradation
4. deposition of particulate contaminants on the ocean and river bed or resuspension from the bed
5. contaminant contribution from outside point and nonpoint sources

Transport of contaminants attached to sediments is simulated separately for those adsorbed by each sediment size fraction.

FETRA also predicts changes in ocean and river bed conditions, including: 1) bed elevation changes due to sediment deposition and scouring, 2) distribution of bed sediment size fractions, and 3) distribution of particulate contaminant concentrations in the bed.

The modified FETRA code was tested to solve several simple equations by using the linear approximation to velocity and depth. Computed results indicate good agreement with analytical solutions. The modified FETRA code was also used to compute sediment transport capacities of wave-induced flows in offshore and surf zones. Through these tests, FETRA demonstrates its applicability to coastal zones and large lakes where wave actions can be one of the dominant mechanisms for transport of sediment and contaminants.

The next step is to verify the FETRA model. This will be accomplished by applying FETRA to coastal zone to simulate migration of sediment and radionuclides and by comparing computer results with field data. The computer printout of FETRA will be released after the model is applied to a coastal zone in FY-1980 to examine the model validity.

In addition, since FETRA has a limited applicability to a stratified estuary, a three-dimensional model is currently being developed to simulate movements of flow, salinity, sediment and contaminants in an estuary.

CONTENTS

LIST OF SYMBOLS

A = the river bed surface area

a' = empirical constant in Equation (29)

a_i = wave amplitude

B = width of the river

B^* = constant in Equation (19)

C_j = concentration of sediment of j^{th} type (weight of sediment per unit volume of water)

$\overline{C}_j$ = depth averaged concentration of sediment for j^{th} type

c_j = fluctuations from the depth averaged concentration of sediment of j^{th} type

$\overline{C}_o$ = bed load concentration

C_{oj} = constant concentration of j^{th} sediment

D = equi[illegible] sediment particle diameter

D_j = diameter of j^{th} sediment

d_m = mean fetch depth

D_x, D_y = dispersion coefficients of x and y directions

E_b = the energy of the breaking waves

$(ECn)_b$ = the energy flux of the waves evaluated at the breaker zone

F_{eff} = effective fetch length

f_{sj} = fraction of contaminant sorbed by j^{th} sediment

f_w = fraction of contaminant left in solution

g = gravitational acceleration

G_{Bj} = particulate contaminant concentration associated with j^{th} sediment in river and ocean bed

G_j = particulate contaminant concentration associated with j^{th} sediment (weight or contaminant per unit weight of sediment)

G_{oj} = constant concentration of particulate contaminate associated with j^{th} sediment

$\bar{G}_w$ = dissolved contaminant concentration (weight of contaminant per unit volume of water

G_w = depth averaged value of pollutant concentration

G_w'' = fluctuation from the depth averaged value of pollutant concentration

G_{wo} = constant concentration of dissolved contaminant

h = flow depth

h_b = water depth at wave breaking

H_s = significant wave height

I_ℓ = immersed weight littoral transport rate

K_{bj} = transfer rate of contaminant with j^{th} non-moving sediment in bed

K_{dj} = distribution (or partition) coefficient between dissolved contaminant and particulate contaminant associated with j^{th} sediment

K_i = wave number

K_j = transfer rate of contaminant for j^{th} moving sediment

K_j = an empirical constant depending on the sediment type

$K_x = \varepsilon_x + D_x$

$K_y = \varepsilon_y + D_y$

M_j = erodibility coefficient for sediment of j^{th} type fraction

M_j = weight of j^{th} sediment

P = probability that the instantaneous lift on the sediment is greater than its submerged weight

POR = porosity of bed sediment

Q_B = bed load

Q_{cj} = lateral influx of j^{th} sediment

Q_j = lateral influx of particulate contaminant adsorbed by j^{th} sediment

Q_S = suspended load

Q_w = lateral influx of dissolved contaminant

S_{Dj} = sediment deposition rate per unit bed surface area for j^{th} sediment type

S_ℓ = volumetric littoral transport

S_{Rj} = sediment erosion rate per unit bed surface area for j^{th} sediment type

t = time

T_s = significant wave period

U = velocity component of longitudinal (x) direction

U = depth averaged longitudinal velocity

$\bar{u}$ = average longitudinal velocity in the boundary layer

u'' = longitudinal velocity fluctuation from the depth averaged longitudinal velocity

U_{AB} = velocity component of incidental flow near the ocean bed

U_B = mass transport velocity of a wave near the ocean bed

U_I = velocity of incidental flow in a surf zone

U_{IS} = velocity component of incidental flow in the interior zone

U_S = mass transport velocity of a wave in the interior zone

U_w = wind velocity

V = velocity component of lateral (y) direction

$\bar{V}$ = depth averaged lateral velocity

v'' = lateral velocity fluctuation from the depth averaged lateral velocity

$\bar{v}_\ell$ = velocity caused by the combination of waves and currents

W = velocity component of vertical (z) direction

W_{sj} = fall velocity of sediment particle of j^{th} type

x,y,z = longitudinal, lateral and vertical direction in Cartesian coordinates, respectively

α_b = wave breaker angle with a shoreline

γ = reentrain coefficient, i.e., probability that particle settling to the bed is reentrained

γ_j = specific weight of j^{th} sediment

γ_s = specific weight of sediment

$\varepsilon_x, \varepsilon_y, \varepsilon_z$ = diffusion coefficients of longitudinal, lateral and vertical directions for j^{th} sediment type

λ = chemical and biological decay rate of contaminant

ν = kinematic viscosity of water

ρ = water density

ρ_s = sediment density

σ = constant

τ_b = bed shear stress

τ_{cDj} = critical shear stress for sediment deposition for j^{th} sediment type fraction

τ_{cRj} = critical shear stress for sediment erosion for j^{th} sediment type fraction

ω = wave frequency

MODIFIED FINITE ELEMENT TRANSPORT MODEL, FETRA, FOR SEDIMENT AND RADIONUCLIDE MIGRATION IN OPEN COASTAL WATERS

Y. Onishi
E. M. Arnold
D. W. Mayer

1. INTRODUCTION

The nuclear energy industry has grown considerably during the past decade, and nuclear power is expected to become one of the major sources of energy to meet the growing demands for energy. Although considerable effort is being made to minimize the release of radioactive wastes into the environment, it is important to assess the potential environmental impact of radionuclide releases. Various pathways exist for exposure of humans and biota to radioactive materials released from nuclear facilities. Hydrologic transport (liquid pathway) is one element in the evaluation of the total radiation dose to man. Exposures can occur from routine or accidental releases of radionuclides in liquid effluents from nuclear facilities. Mathematical models supported by well-planned field data collection programs can be useful tools in assessing the hydrologic transport and ultimate fate of radionuclides.

Many radionuclides found in surface waters originated from effluents discharged from nuclear power plants, waste burial sites and other nuclear-related facilities. These radionuclides are dispersed by stream flows, ocean currents, surface waves and turbulent mixing. However, radionuclides with high distribution coefficients (e.g., cerium, cesium, plutonium which are easily adsorbed by sediment) or radionuclides in surface waters with high suspended sediment concentrations are, to a great extent, adsorbed by river and marine sediments. Thus, otherwise dilute contaminants are concentrated. Contaminated sediments may be deposited on the river and ocean beds creating a significant pathway to man. Contaminated bed sediment may become a long-term source of pollution through desorption and resuspension. In contrast, sorption by sediment can be an important mechanism for reducing the area of influence of these contaminants by reducing concentrations of dissolved constituents.

Field measurements of radionuclide concentrations in the Clinch River indicate that approximately 90% of the ^{137}Cs released was adsorbed by the suspended sediment in the river within 20 miles downstream from the effluent discharge (Churchill et al. 1965). Measurements conducted in the Irish Sea near the Windscale Nuclear Fuel Reprocessing Plant in England indicate that approximately 95% of ^{239}Pu discharged from the plant to the Irish Sea was adsorbed by marine sediment and only 5% remains in solution in sea water (Hetherington 1975). These data also revealed that ^{106}Ru and ^{144}Ce behave in a manner similar to ^{239}Pu. At the other extreme, most of the ^{3}H and ^{90}Sr are in a dissolved form.

In order to assess migration, accumulation and fate of radionuclides and other contaminants (e.g., pesticides, heavy metals, PCB's) in surface waters, mathematical models must include major contaminant transport and fate mechanisms. These mechanisms include:

1. advection and diffusion/dispersion of contaminants
2. degradation and decay of contaminants
3. interaction between sediment and contaminants such as:
   - contaminant adsorption by sediment
   - contaminant desorption from sediment to water
   - transport of particulate contaminants (those adsorbed by sediment)
   - deposition of particulate contaminants to ocean and river beds
   - scouring of particulate contaminants from ocean and river beds
4. contaminant contributions from outside point and nonpoint sources into the system.

Until recently, sediment-contaminant interaction was not included in mathematical models because of the complex nature of sediment transport and contaminant adsorption/desorption mechanisms (Leendertse, 1970, Norton et al. 1974, Onishi 1979). Computer simulation models that calculate contaminant transport without including contaminant-sediment interaction predict that contaminants will be transported in surface waters at the same rate at which water is exchanged. In reality, however, sediment sorption effects would cause some contaminants to migrate much more slowly, at approximately the rate at which the sediment is exchanged in the surface water systems (Haushield et al. 1977, Onishi and Wise 1978, U.S. Environmental Protection Agency 1978). This process may result in a long-term source of pollution through desorption and resuspension of contaminated bed sediments. Hence, in some cases neglecting these sediment effects prohibits accurate prediction of contaminant migration as stated by U.S. Nuclear Regulatory Commission (1973 and 1978).

In order to obtain more realistic predictions of contaminant concentrations in various surface water bodies, the sediment-contaminant transport model, FETRA (Onishi et al, 1976, 1978 and 1979a) was modified to be applicable to open coastal waters where wave actions can be one of the dominant mechanisms to transport sediment and contaminants. FETRA solves transport of sediment and contaminant by including sediment-contaminant interactions. This report describes the formuations of the modified version of FETRA and some computer results of transport rate of sediment suspended and transported by surface waves in offshore and surf zones.

2. MATHEMATICAL MODEL FORMULATION OF MODIFIED FETRA

The modified FETRA code is an unsteady two-dimensional finite element model, utilizing the Galerkin weighted residual method. The model consists of three submodels coupled to include the effects of sediment-contaminant interaction on contaminant transport. The submodels are: 1) sediment transport submodel, 2) dissolved contaminant transport submodel, and 3) particulate contaminant (contaminant adsorbed by sediment) transport submodel.

SEDIMENT TRANSPORT SUBMODEL

The sediment transport submodel solves the migration of sediment (transport, deposition and scouring) for three sediment size fractions of cohesive and noncohesive sediments (e.g., sand, silt and clay) separately, since movement and adsorption capacity vary significantly with sediment size. The model includes the mechanisms of:

1. convection and dispersion of sediment
2. wave motion to suspend sediments
3. fall velocity and cohesiveness
4. deposition on the ocean and river beds
5. resuspension from the ocean and river beds (bed erosion and armoring)
6. sediment contributions from outside point and nonpoint sources to the system.

Sediment mineralogy and water quality effects are implicitly included through the above mentioned mechanisms 3, 4 and 5.

This submodel also calculates changes in ocean and river bed conditions, including bed elevation changes and distribution of sediment size fraction within the bed.

The governing equation of sediment transport for the three-dimensional case is:

$$\frac{\partial C_j}{\partial t} + \frac{\partial}{\partial x}(UC_j) + \frac{\partial}{\partial y}(VC_j) + \frac{\partial}{\partial z}\left\{(W - W_{sj})C_j\right\}$$
$$= \frac{\partial}{\partial x}\left(\varepsilon_x \frac{\partial C_j}{\partial x}\right) + \frac{\partial}{\partial y}\left(\varepsilon_y \frac{\partial C_j}{\partial y}\right) + \frac{\partial}{\partial z}\left(\varepsilon_z \frac{\partial C_j}{\partial z}\right) \qquad (1)$$

where

C_j = concentration of sediment of j^{th} size fraction (weight of sediment per unit volume of water)

t = time

U = velocity component of longitudinal (x) direction

V = velocity component of lateral (y) direction

W = velocity component of vertical (z) direction

W_{sj} = fall velocity of sediment particle of j^{th} type

x,y,z = longitudinal, lateral and vertical directions in Cartesian coordinates, respectively

$\varepsilon_x, \varepsilon_y, \varepsilon_z$ = diffusion coefficients of longitudinal, lateral and vertical directions.

Boundary conditions are:

$$(W - W_{sj})C_j - \varepsilon_z \frac{\partial C_j}{\partial z} = 0 \qquad \text{at } z = h \qquad (2)$$

$$(1-\gamma)\, W_{sj}C_j + \varepsilon_z \frac{\partial C_j}{\partial z} = S_{DJ} - S_{RJ} \qquad \text{at } z = 0 \qquad (3)$$

$$C_j = C_{oj} \quad \text{or} \quad VC_j - \varepsilon_y \frac{\partial C_j}{\partial y} = Q_{cj} \qquad \text{at } y = 0 \text{ and } B \qquad (4)$$

where

B = width of a study area

C_{oj} = constant concentration of j^{th} sediment

h = flow depth

Q_{cj} = lateral influx of j^{th} sediment

S_{Dj} = sediment deposition rate per unit bed surface area for j^{th} sediment size fraction

S_{Rj} = sediment erosion rate per unit bed surface area for j^{th} sediment size fraction

γ = reentrain coefficient, i.e., probability that particle settling to the bed is reentrained.

Since a value of γ is not easily available for various flow conditions, γ was assumed to be unity in this study; that is, for the same flow condition all suspended matter settling on the river and ocean bed by the settling velocity reentrains to the flow. In another word, there are no sediment particle exchange between suspended and bottom sediments under an equilibrium condition of sediment transport. It is also assumed that the vertical flow velocity, W, is negligible.

Let:

$$C_j = \overline{C}_j + c''_j \tag{5}$$

$$U = \overline{U} + u'' \tag{6}$$

$$V = \overline{V} + v'' \tag{7}$$

$$\frac{\partial c''_j}{\partial x} = \frac{\partial c''_j}{\partial y} = \frac{\partial W_{sj}}{\partial z} = 0 \tag{8}$$

where

$\overline{C}_j, \overline{U}, \overline{V}$ = depth averaged values of concentration of sediment for j^{th} size fraction, longitudinal velocity, and lateral velocity, respectively

c''_j, u'', v'' = fluctuations from the depth averaged values of concentration of sediment of j^{th} size fraction, longitudinal velocity, and lateral velocity, respectively.

By substituting the above expressions into Equation (1) and integrating it over the entire flow depth, this equation becomes:

$$\overline{C}_j \left\{ \frac{\partial h}{\partial t} + \frac{\partial}{\partial x}(\overline{U}h) + \frac{\partial}{\partial y}(\overline{V}h) \right\} - (\overline{C}_j + c_j'')\Big|_{z = h} \left\{ \frac{\partial h}{\partial t} + (\overline{U} + u'')\Big|_{z = h} \frac{\partial h}{\partial x} \right.$$

$$\left. + (\overline{V} + v'')\Big|_{z = h} \frac{\partial h}{\partial y} \right\} + \left\{ W_{s_j}(\overline{C}_j + c_j'')\Big|_{z = h} + \varepsilon_z \frac{\partial(\overline{C}_j + c''_j)}{\partial z}\Big|_{z = h} \right\}$$

$$= - h \left(\frac{\partial \overline{C}}{\partial t}j + \overline{U}\frac{\partial \overline{C}}{\partial y}j + \overline{V}\frac{\partial \overline{C}}{\partial y}j \right) + h\frac{\partial}{\partial x}\left(\varepsilon_x \frac{\partial \overline{C}}{\partial x}j \right) + h\frac{\partial}{\partial y}\left(\varepsilon_y \frac{\partial \overline{C}}{\partial y}j \right)$$

$$- \frac{\partial}{\partial x} \int_0^h u''c_j''dz - \frac{\partial}{\partial y} \int_0^h v''c_j dz - \left\{ W_{s_j} (\overline{C}_j + c_j'')\Big|_{z = 0} \right.$$

$$\left. + \varepsilon_z \frac{\partial \overline{C}_j + c_j''}{\partial z}\Big|_{z = 0} \right\} \tag{9}$$

The equation of continuity, the kinetic water surface boundary condition and Equation (2) make the left side of Equation (9) zero. As in the Boussinesq diffusion coefficient concept, let:

$$\int_0^h u''c_j''dz = \overline{(u''c_j'')}h = - hD_x \frac{\partial \overline{C}}{\partial x}j \tag{10}$$

and

$$\int_0^h v''c_j''dz = \overline{(v''c_j'')}h = - hD_y \frac{\partial \overline{C}}{\partial y}j \tag{11}$$

where D_x and D_y equal the dispersion coefficients of x and y directions. Hence, Equations (2), (3), (9), (10), and (11) yield the following final expression of sediment transport:

$$\frac{\partial \overline{C}_j}{\partial t} + \left(\overline{U} - \frac{D_x}{h}\frac{\partial h}{\partial x}\right)\frac{\partial \overline{C}_j}{\partial x} + \left(\overline{V} - \frac{D_y}{h}\frac{\partial h}{\partial y}\right)\frac{\partial \overline{C}_j}{\partial y}$$

$$= \frac{\partial}{\partial x}\left(K_x \frac{\partial \overline{C}_j}{\partial x}\right) + \frac{\partial}{\partial y}\left(K_y \frac{\partial \overline{C}_j}{\partial y}\right) + \frac{S_{Rj}}{h} - \frac{S_{Dj}}{h} \qquad (12)$$

where

$$K_x = \varepsilon_x + D_x$$

$$K_y = \varepsilon_y + D_y$$

The finite element method was used to solve Equations (4) and (12). In order to solve Equations (4) and (12), sediment erosion and deposition rates, S_{Rj} and S_{Dj}, must be evaluated for various water bodies.

Rivers and Estuaries

Sediment erosion and deposition rates are evaluated separately for each sediment size fraction because erosion and deposition characteristics are significantly different for cohesive and noncohesive sediments.

Erosion and deposition of noncohesive sediments (sand and gravel) are affected by the amount of sediment the flow is capable of carrying. For example, if the amount of sand being transported is less than the flow can carry for given hydrodynamic conditions, the current will scour sediment from the river bed to increase the sediment transport rate. This occurs until the actual sediment transport rate becomes equal to the carrying capacity of the flow or until the available bed sediments are all scoured, whichever occurs first. Conversely, the flow deposits sand and gravel if its actual sediment transport rate is above the flow's capacity to carry sediment. Because of its applicability and simplicity, the following DuBoy's formula (Vanoni 1975) which was originally developed for rivers was used to calculate the flow capacity of noncohesive sediment transport, Q_T in rivers and estuaries:

$$Q_T = B \, \psi_D \, \tau_b \, (\tau_b - \tau_c) \qquad (13)$$

where

B = entire river width or a portion of it

τ_b = bed shear stress

τ_c = critical bed shear stress at which sediment movement begins.

ψ_D = coefficient.

The flow capacity, Q_T, was then compared with the actual amount of sand, Q_{Ta}, being transported in the water. Hence:

$$S_{Rj} = \frac{Q_T - Q_{Ta}}{A} \tag{14}$$

$$S_{Dj} = \frac{Q_{Ta} - Q_T}{A} \tag{15}$$

where

A = entire river and ocean bed surface area or a portion of it.

For sediment erosion and deposition rates of cohesive sediments (silt and clay), the following Partheniades (1962) and Krone (1962) formulas were adopted:

$$S_{Rj} = M_j \left(\frac{\tau_b}{\tau_{cR_j}} - 1 \right) \tag{16}$$

$$S_{Dj} = W_{sj} C_j \left(1 - \frac{\tau_b}{\tau_{cD_j}} \right) \tag{17}$$

where

M_j = erodibility coefficient for sediment of j^{th} size fraction

τ_{cD_j} = critical shear stress for sediment deposition for j^{th} sediment size fraction

τ_{cR_j} = critical shear stress for sediment erosion for j^{th} sediment fraction.

Values of M_j, τcD_j and τcR_j must be determined by field and/or laboratory tests. These values selected for the Columbia River (Washington) and the Clinch River (Tennessee) and Four Mile and Wolf Creeks (Iowa) were reported in recent mathematical simulation studies concerning sediment, radionuclide and pesticide transport in these four rivers simulated by another sediment-contaminant transport model SERATRA (Onishi 1977; Onishi et al. 1979b,c,d). The actual amount of cohesive sediment erosion is the amount calculated by Equation (14) or the total amount of available bed sediment for scouring, whichever is smaller.

When the fall velocity, W_{sj}, depends on sediment concentration, the fall velocity may be assumed (Krone 1972):

$$W_{s_j} = K_j' C_j^{4/3} \tag{18}$$

where

K_j' = an empirical constant depending on the sediment type.

The applicability of Equations 13 through 17 to the James River estuary was shown in Onishi and Wise (1978).

Oceans and Large Lakes With Surface Waves

In most environments occuring in coastal areas and large lakes (e.g., the Great Lakes), marine and lake sediments are mostly suspended by waves which themselves can transport only small amounts of suspended sediment. The sediment suspended by wave action is then transported mostly by a current which, in most cases, is too small to suspend sediment by itself.

Similar to the computation of the erosion and deposition rates of noncohesive sediments in rivers and estuaries, the following cocept was used: If the amount of sand being transported is less than what the flow and wave can carry, the current and waves will scour sediment from the ocean and lake bed to increase the sediment transport rate. The scouring occurs until an actual sediment load is equal to the carrying capacity of the flow and waves or until the available bed sediments are all scoured, whichever occurs first. Conversely, the flow deposits sand if its actual sediment load is above the flow and wave capacity to carry sediment.

When surface waves are present, it is assumed that wave motion is a dominant mechanism for suspension of sediment which will then be transported by a combination of an ambient velocity of incidental flow (those other than one included by wave motion) and the second order velocity components of waves. In this case, the DuBoy's formula for calculating transport of noncohesive sediment in rivers and estuaries was replaced by appropriate wave-sediment transport formulas for offshore and surf zones, as are presented below. Because of the lack of formulations to calculate rates of the cohesive sediment erosion and deposition by waves, Partheniades and Krone's formulas (Equations 16 and 17) for cohesive sediment were used for the marine environment. Since these two formulas were originally developed for estuaries and have not been tested in coastal zones, selection of M, τcD_j and τcR_j must be performed with a great care through model calibration.

Offshore Zone: With the wave energy spectrum as a starting point, results obtained by Einstein (1972) and Liang and Wang (1973) were used to obtain the wave induced sediment suspension in offshore zones. Both the wave-induced bed load and suspended sediment concentrations are calculated. For the bed load the following approach was used: The probability that a sediment particle is set into motion is the same as the probability that the instantaneous lift on the particle is greater than its submerged weight. This probability, denoted by p, is given as follows (Liang and Wang 1973):

$$p = \frac{1}{\sqrt{2\pi}} \int_{B^{\star}\psi - 1/\zeta o}^{\infty} e^{-z^2/2} \, dz \qquad (19)$$

where

$$\psi = \frac{(\rho_s - \rho)}{\rho \bar{u}^2} \; gD$$

$B^* = 4$

$1/\zeta o = 1.5$

ρ_s = sediment density

ρ = water density

γ_s = unit weight of sediment

g = gravitational acceleration

D = equivalent sediment particle diameter

$\overline{u}$ = average horizontal velocity in the boundary layer.

The average bed concentration, $\overline{C}_o$, is given by the following equation

$$\overline{C}_o = A_o p \gamma_s \tag{20}$$

where A_o is a constant which must be determined by experiment. Thus, with a known A_o value, $\overline{C}_o$ can be calculated if u is known (see the expression for ψ).

The velocity $\overline{u}$ is obtained by treating the flow field in the turbulent boundary layer as a superposition of all the components in the random wave train. Thus, $\overline{u}^2$ can be written as:

$$\overline{u}^2 = \sum_i (u_{oi}^2)\ (1 - 2\ f_{1i} \cos f_{2i} + f_{1i}^2) \tag{21}$$

where

$$f_{1i} = 0.5 \exp\left(\frac{-133 \sinh (k_i h)\ z}{a_i\ {}_iD}\right)$$

$$f_{2i} = 0.3\ (\beta_i z)$$

$$\beta_i = \frac{\omega_i}{2\nu}$$

a_i = wave amplitude

ω_i = wave frequency (rad/sec)

h = water depth

k_i = wave number

z = vertical coordinate

$u_{oi} = a_i\omega_i/\sinh(k_i h)$

ν = kinematic viscosity of water.

The average bed load transport Q_B is obtained by integrating as follows:

$$Q_B = \overline{C_o} \int_o^{2D} (U_B + U_{AB})\, dz \tag{22}$$

where

U_{AB} = velocity component of incidental flow (those other than one induced by a wave action) near the ocean bed

U_B = mass transport velocity (second order velocity components) of a wave near the ocean bed.

U_B is calculated by an expression obtained by Liang and Wang (1973). The distribution of vertical velocity, U_{AB}, of the incidental flow is assumed to follow the 1/7-th-power law (Schlichting 1968). Hence, the bed load is transported by both wave induced velocity and the incidental flow.

The concentration of the suspended sediment is calculated by taking the time average of the diffusion equation and solving a resulting linear elliptic equation obtained by neglecting the molecular diffusion coefficient and estimating the diffusion coefficients of wave motion and turbulence. The suspended sediment concentration at elevation z with no depth restriction is given by (Liang and Wang 1973).

$$\frac{C}{\overline{C}_o} = \left[\frac{\tanh(kz/2)}{\tanh(kz_o/2)}\right]^{R_i}, \qquad z_o = 2D \tag{23}$$

$$R_i = \frac{W_s \sinh k_i h}{\gamma\sigma k_i\, a_i\, \omega_i} \tag{24}$$

where

ω_i = frequency

h = water depth

k_i = wave number

$\gamma = 3/(2\ \rho_s/\rho + 1)$

σ = constant

a_i = wave amplitude

W_s = sediment settling velocity

z = vertical coordinate.

For the case of shallow water, the suspended sediment concentration C at the elevation z is given by (Liang and Wang 1973):

$$\frac{C}{\overline{C}_o} = \left(\frac{2D}{z}\right)^{|R_i|} \tag{25}$$

$$R_i = \frac{W_s h}{\gamma \sigma a_i w_i} \tag{26}$$

For this study, Equations (25) and (26) for a shallow water case are used. The rate of suspended sediment transport in the interior zone (Q_S) is then obtained as:

$$Q_S = \int_{2D}^{h} C\ (U_S + U_{IS})\ dz \tag{27}$$

where

U_{IS} = velocity component of incidental flow (those other than one induced by wave action) in the interior zone

U_S = mass transport velocity (second order velocity component) of a wave in the interior zone.

The mass transport velocity, U_S, is calculated by Liang and Wang's expression (Liang and Wang 1973). The vertical velocity distribution of the incidental flow, U_{IS}, is assumed to follow the 1/7-th-power law. Hence, suspended sediment is also transported by both wave-induced velocity and the incidental flow.

Hence, the sediment transport capacity of flow for noncohesive sediment, Q_T, is:

$$Q_T = Q_B + Q_S \tag{28}$$

Q_T, thus obtained, can then be used to calculate the erosion and/or deposition rates of sand by Equations (14) and (15).

Surf Zone: The formulations discussed above are only applicable to regions well beyond the surf zone. The following expressions are used in the FETRA code to include the littoral (longshore) transport of sediments in the surf zone induced by the energy and momentum expended by breaking waves. The work of Komar (1977) and some of his associates was adopted for this study. The volumetric littoral transport rate S and the immersed weight littoral transport rate I_ℓ are given:

$$S_\ell = \frac{I_\ell}{(\rho_s - \rho)\, ga'} \tag{29}$$

$$I_\ell = 0.28\ (ECn)_b \frac{\overline{v}_\ell}{u_m} \tag{30}$$

$$u_m = \left[\frac{2E_b}{\rho h_b}\right]^{1/2} \tag{31}$$

where

$(ECn)_b$ = the energy flux of the waves evaluated at the breaker zone

E_b = the energy of the breaking waves

h_b = the water depth at breaking

$\overline{v}_\ell$ = velocity caused by the combination of waves and currents, $(\overline{v}_\ell = 2.7\ U_m \sin\alpha_b \cos\alpha_b + U_I)$

α_b = breaker angle with the shoreline

U_I = velocity of incidental flow (those other than one induced by waves) in a surf zone, and

a' = an empirical constant ($\approx$0.6).

In the case where the mass transport is induced by wave action alone (in the absence of other currents, i.e., $U_I = 0$), the longshore velocity becomes:

$$\overline{v}_\ell = 2.7U_m \sin\alpha_b \cos\alpha_b \qquad (32)$$

Hence, the transport rates for this particular case are given by:

$$S_\ell = (6.85 \times 10^{-5})\ (EC_n)_b \sin\alpha_b \cos\alpha_b \qquad (33)$$

$$I_\ell = 0.77\ (EC_n)_b \sin\alpha_b \cos\alpha_b \qquad (34)$$

Therefore, the total sediment transport capacity, Q_T, is then calculated by:

$$Q_T = a \cdot S_\ell \qquad (35)$$

where a = unit conversion constant.

Rates of erosion and deposition of noncohesive sediment in a surf zone are then calculated by Equations (14) and (15).

In order to use the above formulas for the offshore and littoral transport of sediment, temporal and spacial variations of wave characteristics, including the wave angle at breaking α_b must be calculated. This was accomplished with 1) inclusion of wind-induced wave mechanisms in FETRA and 2) a wave refraction program which is used in conjunction with FETRA.

For calculation of wave characteristics induced by wind, FETRA uses the following empirical formulations (U.S. Army Corps of Engineers 1962): Waves generated by wind over fetches of known lengths can be computed by a method reported in Sverdrup and Munk (1947), Bretschneider (1953), and the Coastal Engineering Research Center's, "Shore Protection Manual (U.S. Corps of Engineers, 1973).

$$H_s = \frac{0.283\, U_w^2}{g} \tanh\left[0.530\left(\frac{gd_m}{U_w^2}\right)^{0.75}\right] \tanh\left\{\frac{0.0125\left(\frac{g\, F_{eff}}{U_w^2}\right)^{0.42}}{\tanh\left[0.530\left(\frac{gd_m}{U_w^2}\right)^{0.75}\right]}\right\} \quad (36)$$

$$T_s = \frac{1.2\,(2\pi\, U_w)}{g} \tanh\left[0.833\left(\frac{gd_m}{U_w^2}\right)^{0.375}\right] \tanh\left\{\frac{0.077\left(\frac{g\, F_{eff}}{U_w^2}\right)^{0.25}}{\tanh\left[0.833\left(\frac{gd_m}{U_w^2}\right)^{0.375}\right]}\right\} \quad (37)$$

where

H_s = significant wave height (feet)
U = wind velocity (feet per second)
g = acceleration due to gravity (32.2 ft/sec^2)
d_m = mean fetch depth (feet)
F_{eff} = effective fetch length (feet)
T_s = significant wave period (seconds)

The significant wave height, H_s is defined as the average of the one-third highest waves and can be related to the maximum wave height (H_{max}), highest one percent (H_1) and highest ten percent (H_{10}) waves by the following relationships (U.S. Corps of Engineers 1973).

$$H_{max} = 1.77\ H_s$$
$$H_1 = 1.67\ H_2$$
$$H_{10} = 1.27\ H_s$$

The wave amplitude, a, was calculated by:

$$H_{RMS} = H_s/1.416 \qquad (38)$$

$$a = H_{RMS}/2 \qquad (39)$$

The wave number was calculated by Equation (41) through an iteration process.

$$\omega = \frac{2\pi}{T_s} \qquad (40)$$

$$k = \omega^2/\left(g\ .\ \text{Tanh}\ (k\ d_m)\right) = \frac{2\pi}{L} \qquad (41)$$

where

ω = wave frequency

k = wave number

L = wave length

The other method to obtain the necessary wave characteristics is to use the wave refraction program in conjunction with FETRA. This program was developed by Dobson (1967), and later modified by Ecker and Degraca (1974). The theoretical basis of the wave refraction program is derived from geometrical optics and utilizes the Snell's Law. The program utilizes wave hindcast data to obtain the representative deepwater waves for all wave directions and periods. From these deepwater waves, the program simulates the process by which each appropriate deepwater wave ray is generated towards shore. Starting from a known point on a contour grid with a given period and an initial direction, the computer program constructs a single wave ray step by step across the grid. At wave breaking, the program calculates the refraction coefficient, K_R; shoaling coefficient, K_s; the wave angle at breaking, α_b; the depth at breaking, d_b; and the wave height, h_b. The program also computes the alongshore component of wave power at designated stations along the shoreline. The wave characteristics thus obtained by the wave refraction program are then used by FETRA.

DISSOLVED CONTAMINANT TRANSPORT MODEL

The association of dissolved contaminants (such as radionuclides, heavy metals, pesticides and nutrients) with sediments is assumed to be the primary mechanism of contaminant uptake. Consequently, the model includes the effects of:

1. convection and dispersion of dissolved contaminant
2. adsorption (uptake) of dissolved contaminant by sediments (cohesive and noncohesive sediments) or desorption from the sediments into water
3. radionuclide decay or other chemical and biological decay of contaminant
4. contaminant contributions from point and nonpoint sources to the system (e.g., contaminant contributions from wastewater discharges, overland runoff flow, fallout and ground water seepage to a surface water system).

Effects of water quality (e.g., pH, water temperature, salinity, etc.) and sediment characteristics (e.g., clay minerals) are taken into account through changes in the distribution (or partition) coefficient, K_{dj}, and transfer rate, K_j, as shown in the last term of Equation (42).

The governing equation of dissolved contaminant transport for the three-dimensional case is:

$$\frac{\partial G_w}{\partial t} + \frac{\partial}{\partial x}(UG_w) + \frac{\partial}{\partial y}(VG_w) + \frac{\partial}{\partial z}(WG_w)$$

$$= \frac{\partial}{\partial x}\left(\varepsilon_x \frac{\partial G_w}{\partial x}\right) + \frac{\partial}{\partial y}\left(\varepsilon_y \frac{\partial G_w}{\partial y}\right) + \frac{\partial}{\partial z}\left(\varepsilon_z \frac{\partial G_w}{\partial z}\right)$$

$$- \lambda G_w - \sum_j K_j C_j (K_{dj} G_w - G_j) \tag{42}$$

In addition to the previously defined symbols:

K_{dj} = distribution (or partition) coefficient between dissolved contaminant and particulate contaminant associated with j^{th} sediment

K_j = transfer rate of contaminant for j^{th} sediment

G_j = particulate contaminant concentration associated with j^{th} sediment (weight or contaminant per unit weight of sediment)

G_w = dissolved contaminant concentration (weight of contaminant per unit volume of water)

λ = radionuclide, chemical and biological decay rates of contaminant

Distribution coefficient, K_{dj}, is defined by:

$$K_{dj} = \frac{f_{sj}/M'_j}{f_w/V_w} = \frac{f_{sj}}{f_w C_j} \qquad (43)$$

where

f_{sj} = fraction of contaminant sorbed by j^{th} sediment

f_w = fraction of contaminant left in solution

M'_j = weight of j^{th} sediment

V_w = volume of water

$$\frac{f_{sj}}{f_w} = \frac{C_j G_j}{G_w}$$

Hence Equation (43) may be rewritten as:

$$G_j = K_{dj}\, G_w \qquad (44)$$

The adsorption of contaminant by sediments or desorption from the sediments is assumed to occur toward an equilibrium condition with the transfer rate, K_j, if the particulate contaminant concentration differs from its equilibrium values as expressed in Equation (44).

Literature review on adsorption/desorption mechanism revealed that a most common way to express this mechanism is to use a distribution coefficient, K_d. A distribution coefficient is a function of many parameters, including radionuclide chemical state, water quality of a receiving water body, sediment sizes and clay minerals, and organic content. Unfortunately, the present knowledge on K_d is not advanced enough to determine these functional relationships. Hence in this model, values of K_d will be assigned to the model as input data reflecting effects of these influencing variables. Actual K_d and K_j values with j^{th} sediment may be obtained from field measurements or laboratory tests.

The boundary conditions for dissolved contaminant transport are:

$$WG_w - \varepsilon_z \frac{\partial G_w}{\partial z} = 0 \qquad \text{at } z = h \qquad (45)$$

$$\varepsilon_z \frac{\partial G_w}{\partial z} = \sum_j \gamma_j \, (1\text{-POR}) \, D_j \, K_{bj}(K_{bj}G_w - G_{BJ}) \qquad \text{at } z = 0 \qquad (46)$$

$$VG_w - \varepsilon_y \frac{\partial G_w}{\partial y} = Q_w \quad \text{or} \quad G_w = G_{wo} \qquad \text{at } y = 0 \text{ and } B \qquad (47)$$

where

D_j = diameter of j^{th} sediment

G_{Bj} = particulate contaminant concentration per unit weight of sediment in j^{th} sediment size fraction in the bed

G_{wo} = constant concentration of dissolved contaminant

K_{bj} = transfer rate of contaminants with j^{th} non-moving sediment in bed

POR = porosity of bed sediment

Q_w = lateral influx of dissolved contaminant

γ_j = specific weight of j^{th} sediment

Equation 46 expresses that there is direct adsorption or desorption of contaminant between dissolved contaminant and non-moving bed sediment. It was assumed that a contaminant has the same distribution coefficient values, K_{dj}, for the moving (suspended and bed load sediments) and not moving (bed sediment without any motion) j^{th} sediment. However, these two types of sediments have different transfer rates, K_j and K_{bj}, as expressed in Equations 42 and 46.

Let:

$$G_w = \overline{G}_w + G''_w \tag{48}$$

$$\frac{\partial G''_w}{\partial x} = \frac{\partial G''_w}{\partial y} = 0 \tag{49}$$

where

$\overline{G}_w$ = depth averaged value of pollutant concentration

G_w = fluctuation from the depth averaged value of pollutant concentration

By substituting the above expressions with those in Equations (5) through (8), into Equation (42) and integrating it over the entire flow depth, Equation (42) becomes:

$$\bar{G}_w \left\{\frac{\partial h}{\partial t} + \frac{\partial}{\partial x}(\bar{U}h) + \frac{\partial}{\partial y}(\bar{V}h)\right\} - (\bar{G}_w + G_w'')\Big|_{z=h}\left\{\frac{\partial h}{\partial t} + (\bar{U} + u'')\Big|_{z=h}\frac{\partial h}{\partial x}\right.$$

$$\left. + (\bar{V} + v')\Big|_{z=h}\frac{\partial h}{\partial y}\right\} + \left\{(\bar{W} + w'')(\bar{G}_w + G_w'')\Big|_{z=h} - \varepsilon_z\frac{\partial}{\partial z}(\bar{G}_w + G_w'')\Big|_{z=h}\right\}$$

$$= - h\left\{\frac{\partial \bar{G}_w}{\partial t} + \bar{U}\frac{\partial \bar{G}_w}{\partial x} + \bar{V}\frac{\partial \bar{G}_w}{\partial y} + D_x\frac{\partial h}{\partial x}\frac{\partial \bar{G}_w}{\partial x} + D_y\frac{\partial h}{\partial y}\frac{\partial \bar{G}_w}{\partial y}\right\}$$

$$+ h\frac{\partial}{\partial x}\left\{(\varepsilon_x + D_x)\frac{\partial \bar{G}_w}{\partial x}\right\} + h\frac{\partial}{\partial y}\left\{(\varepsilon_y + D_y)\frac{\partial \bar{G}_w}{\partial y}\right\}$$

$$- \lambda h\bar{G}_w - h\sum_j K_j\bar{C}_j(K_{dj}\bar{G}_w - G_j) - \varepsilon_z\frac{\partial}{\partial z}(\bar{G}_w + G_w'')\Big|_{z=o} \qquad (50)$$

The equation of continuity, the kinetic water surface boundary condition and boundary condition shown in Equation (45) then make the left side of Equation (50) zero. Hence, the final transport equation of dissolved contaminant is:

$$\frac{\partial \bar{G}_w}{\partial t} + (\bar{U} - \frac{D_x}{h}\frac{\partial h}{\partial x})\frac{\partial \bar{G}_w}{\partial x} + (\bar{V} - \frac{D_y}{h}\frac{\partial h}{\partial y})\frac{\partial \bar{G}_w}{\partial y} = \frac{\partial}{\partial x}(k_x\frac{\partial \bar{G}_w}{\partial x}) + \frac{\partial}{\partial y}(k_y\frac{\partial \bar{G}_w}{\partial y})$$

$$- (\lambda + \sum_j K_j K_{dj}\bar{C}_j - \frac{1}{h}\sum_j \gamma_j(1\text{-POR})D_j K_{bj}K_{dj})G_w$$

$$+ \sum_j K_j\bar{C}_j G_j - \frac{1}{h}\sum_j \gamma_j(1\text{-POR})D_j K_{bj}G_{Bj} \qquad (51)$$

The boundary conditions for this equation are those in Equation (47).

PARTICULATE CONTAMINANT TRANSPORT MODEL

The transport model of contaminants attached to sediments is solved separately for those adsorbed by each sediment size fraction of cohesive and noncohesive sediments. This model also includes the mechanisms of:

1. convection and dispersion of particulate contaminant
2. adsorption (uptake) of dissolved contaminant by sediments or desorption from sediments into water
3. radionuclide, chemical and biological decay of contaminant
4. deposition of particulate contaminant on the ocean and river beds or resuspension from the beds
5. contaminant contributions from point and nonpoint sources to the system (e.g., contaminant contributions from wastewater discharges, overland runoff flow, fallout and ground water to a surface water system).

As in the transport of sediments and dissolved contaminant, the three-dimensional transport equation for contaminants adsorbed by the j^{th} sediment size may be expressed as:

$$\frac{\partial C_jG_j}{\partial t} + \frac{\partial}{\partial x}(UC_jG_j) + \frac{\partial}{\partial y}(VC_jG_j) + \frac{\partial}{\partial z}\left\{(W - W_{s_j})C_jG_j\right\} = \frac{\partial}{\partial x}\left(\varepsilon_x \frac{\partial C_jG_j}{\partial x}\right)$$

$$+ \frac{\partial}{\partial y}\left(\varepsilon_y \frac{\partial C_jG_j}{\partial y}\right) + \frac{\partial}{\partial z}\left(\varepsilon_z \frac{\partial C_jG_j}{\partial z}\right) - \lambda C_jG_j - K_jC_j(G_j - K_{dj} G_w) \qquad (52)$$

where the particulate contaminant concentration, G_j, is assumed to be independent of z as reported by Onishi et al. (1979b,c,d). All symbols in Equation (52) were previously defined. Noting Equations (2), (3), and (4), the boundary conditions for this case become:

$$(W - W_{sj}) G_jG_j - \varepsilon_z \frac{\partial C_jG_j}{\partial z} = G_j \left\{(W-W_{sj}) C_j - \varepsilon_z \frac{\partial C_j}{\partial z}\right\} = 0 \quad \text{at } z = h \qquad (53)$$

$$(1-\gamma)\; W_{sj}C_jG_j + \varepsilon_z \frac{\partial C_jG_j}{\partial z} = G_jS_{Dj} - G_{Bj}S_{Rj} \qquad \text{at } z = 0 \qquad (54)$$

$$G_j = G_{jo} \quad \text{or} \quad VC_j\; G_j - \varepsilon_y \frac{\partial C_jG_j}{\partial y} = Q_j \qquad \text{at } y = 0 \text{ and } B \qquad (55)$$

where

G_{Bj} = a particulate contaminant concentration associated with j^{th} sediment in ocean or river bed

G_{oj} = constant concentration of particulate contaminant

Q_j = lateral influx of particulate contaminant

Equation (56) is derived by 1) substituting Equations (5) through (8) into Equation (52), 2) integrating it over the flow depth, 3) then substrating equation Equation (9) multiplied by G_j from the resulting equation, and 4) substituting the boundary conditions, Equations (53) and (54):

$$\frac{\partial G_j}{\partial t} + \left\{ \overline{U} - \frac{2\varepsilon_x}{\overline{C}_j}\frac{\partial \overline{C}_j}{\partial x} - \frac{D_x}{\overline{C}_j}\frac{\partial \overline{C}_j}{\partial x} + \frac{\varepsilon_x}{\overline{C}_j h}\frac{\partial h}{\partial x}\, c_j''\Big|_{z=h} \right\} \frac{\partial G_j}{\partial x}$$

$$+ \left\{ \overline{V} - \frac{2\varepsilon_y}{\overline{C}_j}\frac{\partial \overline{C}_j}{\partial y} - \frac{D_y}{\overline{C}_j}\frac{\partial \overline{C}_j}{\partial y} + \frac{\varepsilon_y}{\overline{C}_j h}\frac{\partial h}{\partial y}\, c_j''\Big|_{z=h} \right\} \frac{\partial G_j}{\partial y}$$

$$= \frac{\partial}{\partial x}\left(\varepsilon_x \frac{\partial G_j}{\partial x}\right) + \frac{\partial}{\partial y}\left(\varepsilon_y \frac{\partial G_j}{\partial y}\right) - \left(\frac{S_{Rj}}{\overline{C}_j h} + \lambda + K_j\; G_j\right)$$

$$+ \left(K_j\; K_{dj}\; G_w + \frac{G_{Bj}\; S_{Rj}}{\overline{C}_j h}\right) \qquad (56)$$

Since the two terms containing c_j'' in the above equation are at least one order of magnitude smaller than the rest of the terms, these two terms may be omitted. Hence, the final expression becomes:

$$\frac{\partial G_j}{\partial t} + \left\{ \overline{U} - \frac{2\varepsilon_x}{\overline{C}_j} \frac{\partial \overline{C}_j}{\partial x} - \frac{D_x}{\overline{C}_j} \frac{\partial \overline{C}_j}{\partial x} \right\} \frac{\partial G_j}{\partial x} + \left\{ \overline{V} - \frac{2\varepsilon_y}{\overline{C}_j} \frac{\partial \overline{C}_j}{\partial y} - \frac{D_y}{\overline{C}_j} \frac{\partial \overline{C}_j}{\partial y} \right\} \frac{\partial G_j}{\partial y}$$

$$= \frac{\partial}{\partial x} \left(\varepsilon_x \frac{\partial G_j}{\partial x} \right) + \frac{\partial}{\partial y} \left(\varepsilon_y \frac{\partial G_j}{\partial y} \right) - \left(\frac{S_{Rj}}{\overline{C}_j h} + \lambda + K_j \; G_j \right)$$

$$+ \left(K_j \, K_d \;\; G_w + \frac{G_{Bj} S_{Rj}}{\overline{C}_j h} \right) \qquad (57)$$

The boundary conditions for this case are those expressed in Equation (55).

FINITE ELEMENT METHOD

Because of its increased solution accuracy and ready accommodation to various boundary geometrics, the finite element method was selected for this study. The finite element solution technique with the Galerkin weighted residual method was used to solve Equations (12), (51) and (57) with the boundary conditions of Equations (4), (47) and (55).

The flow domain is divided into a series of triangular elements interconnected at nodal points. Six nodes are associated with each triangle, three at the vertices called corner nodes and three on the mid-sides called mid-side nodes. A quadratic approximation is made for the sediment and contaminant concentrations within each element. One important consideration to the model formulation is the compatibility of FETRA to a hydrodynamic model which provides input data of velocity and depth to FETRA. From the standpoint of compatibility to FETRA, these hydrodynamic distributions can best be obtained by an unsteady, two-dimensional, finite element model, such as CAFE developed by Pagenkopf et al. (1976) and RMA II developed by Norton et al. (1974). In order for FETRA to be compatible with various hydrodynamic codes, the modified FETRA use either linear (with three nodal points) or quadratic (with six nodal points) interpolation for the variations of flow depth and velocity within a triangular element.

DATA REQUIREMENTS OF FETRA

All of the input data required to operate FETRA are listed below for each submodel of FETRA:

All submodels:

- Channel geometry or bathymetry
- Depth and velocity distributions which will be obtained by a hydrodynamic code (e.g., RMA II or CAFE) with field data
- Longitudinal and lateral dispersion coefficients.

Sediment transport model:

- Sediment size distribution
- Sediment density and fall velocity
- Critical shear stresses of erosion and deposition of cohesive sediments (silt and clay)
- Erodibility coefficient for erosion of cohesive sediment
- For marine environments

  a) Wave characteristics of deep water

     Wave number
     Wave height
     Wave frequency
     Direction of wage propagation

These wave characteristics are used to calculate wave angles in a study area by the Wave Refraction model. Computed wave characteristics in the study area will then be used for FETRA to simulate sediment-wave interaction.

b) Information for wind-generated waves
   Wind velocity
   Mean fetch depth
   Effective fetch length

- Initial conditions

  Sediment concentrations for each sediment size fraction
  Bottom sediment size fraction

- Boundary conditions

  Sediment concentration or lateral influx of sediment at the boundaries

Dissolved and particulate contaminant transport submodels:

- Distribution coefficients of contaminants with river and marine sediments for each sediment size fraction

- Initial conditions

  Dissolved contaminant concentration

  Particulate contaminant concentration associated with sediment in water for each sediment size fraction

  Particulate contaminant concentration for each sediment size fraction within ocean and river bed

- Boundary conditions

  Dissolved contaminant concentration or lateral influx of dissolved contaminants at the boundaries

  Particulate contaminant concentration or lateral influx of particulate contaminant at the boundaries for each sediment size fraction.

Concentrations of sediments and particulate contaminant associated with each sediment size fraction as initial and boundary conditions are required. However, if these detailed data are not available, they may be estimated by a concentration of bulk sediment and a particulate contaminant concentration attached to bulk sediment, with the sediment size distribution and distribution coefficient of contaminant.

OUTPUT OF FETRA

The FETRA code then computes the following:

Sediment simulation for any given time:

- longitudinal and lateral distributions of total sediment (sum of suspended and bed load) concentration for each sediment size fraction
- three-dimensional (longitudinal, lateral and vertical) distributions of sediment size fraction in the ocean and river bed
- change in bed elevation (elevation changes due to sediment deposition and/or scour)

Contaminant simulation for any given time:

- longitudinal and lateral distributions of dissolved contaminant concentration
- longitudinal and lateral distributions of contaminant concentration adsorbed by sediment for each sediment size fraction
- three-dimensional distributions of contaminant concentrations in the bottom sediment within the bed for each sediment size fraction.

MODELING PROCEDURE

The modeling procedure of contaminant migration in rivers, estuaries, oceans and large lakes is shown in Figure 1. The sequence of modeling is shown by the direction of the arrows. As indicated in this figure, the procedure consists of the following three steps:

Step 1. "Field Data Collection" to supply necessary input data to various mathematical models.

Step 2. "Mathematical Modeling" consisting of the following substeps to simulate river flows, tidal flows, ocean currents, waves and transport of sediment and contaminants.

2.1 "Hydrodynamic Modeling by a hydrodynamic code, e.g., RMA II or CAFE" to obtain velocity and depth distributions

2.2 "Wave Dynamic Modeling by Wave Refraction Model" to predict temporal and spatial distributions of wave characteristics for marine and large lacustrine environments.

2.3 "Sediment and Contaminant Transport by FETRA" which consists of the following four simulations performed by the model, FETRA, internally.

2.3.1 "Sediment Transport Modeling" involving sediment transport simulation.

2.3.2 "Dissolved Contaminant Transport Modeling" to simulate dissolved contaminant movement by including the interaction with sediments.

2.3.3 "Particulate Contaminant Transport Modeling" to simulate particulate contaminant movements by including the interaction with dissolved contaminant and sediments.

2.3.4 "Ocean Bed Modeling" to simulate changes in river and ocean bed conditions including: 1) river and ocean bed elevation change, 2) distribution of sediment size fraction in the bed, and 3) distribution of particulate contaminants within the bed.

Step 3. "Analysis of Computer Results" to assess migration of contaminants.

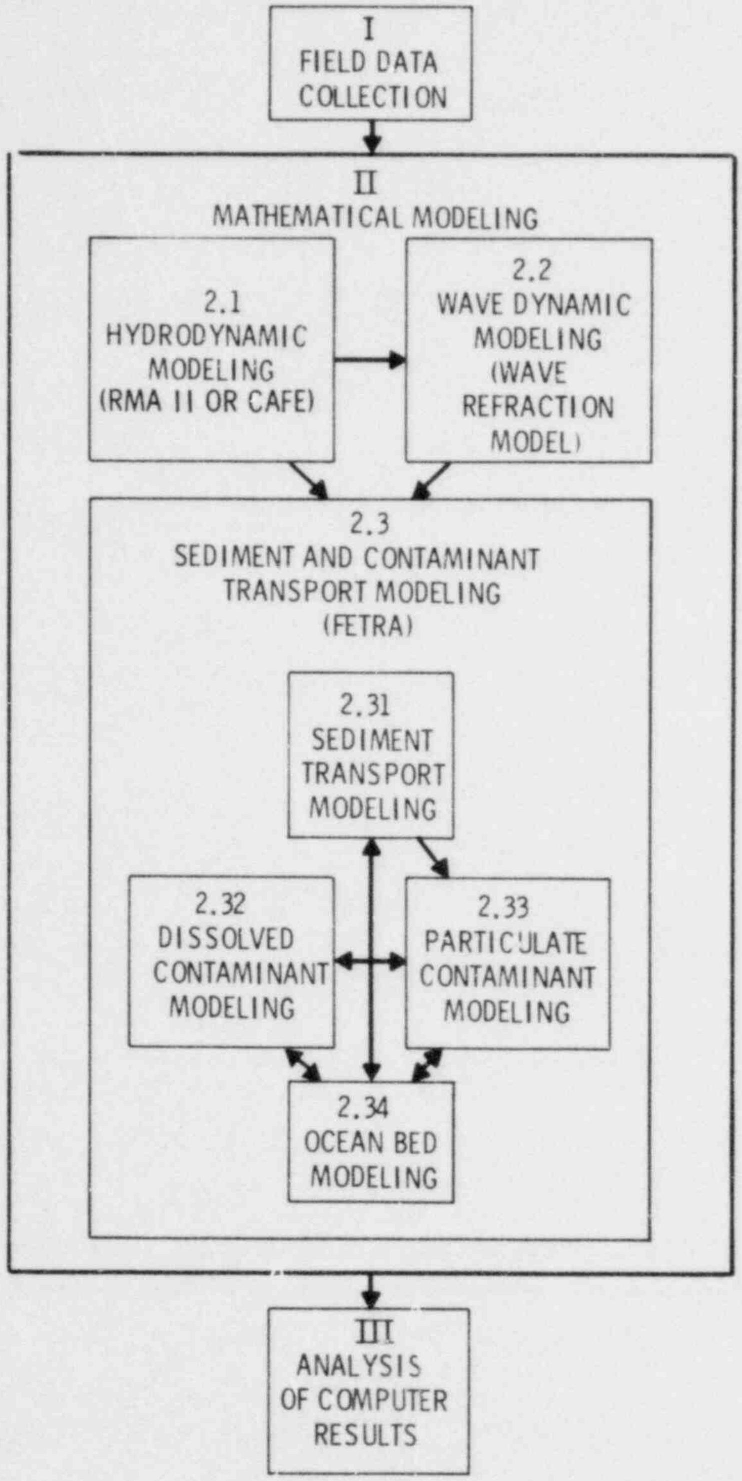

FIGURE 1. Modeling Procedure

3. EXAMINATION OF BASIC COMPUTATIONAL SCHEME

The accuracy and convergence of the numerical solutions calculated by the modified FETRA were evaluated to examine the basic finite element computational scheme of the model. Various simple equations were solved by FETRA and computer results were then compared with known analytical solutions. In this report, the following three examples by using the linear approximation to velocity and depth are discussed:

Example 1

In the first example, the following one-dimensional, steady convection-diffusion equation with a decay term was solved:

$$U \frac{dC}{dx} = \varepsilon_x \frac{d^2C}{dx^2} - \alpha C$$

With the boundary conditions of:

$$C = C_o \qquad \text{at } x = 0$$

$$\frac{dC}{dx} = 0 \qquad \text{at } x = \ell$$

Figure 2 shows computed results and analytical solution, assuming:

$$U = 5.0,\ \varepsilon_x = 0.2,\ \alpha = 10.0,\ C_o = 1.0 \text{ and } \ell = 1.0.$$

The figure indicates a very good agreement between computed and analytical solutions.

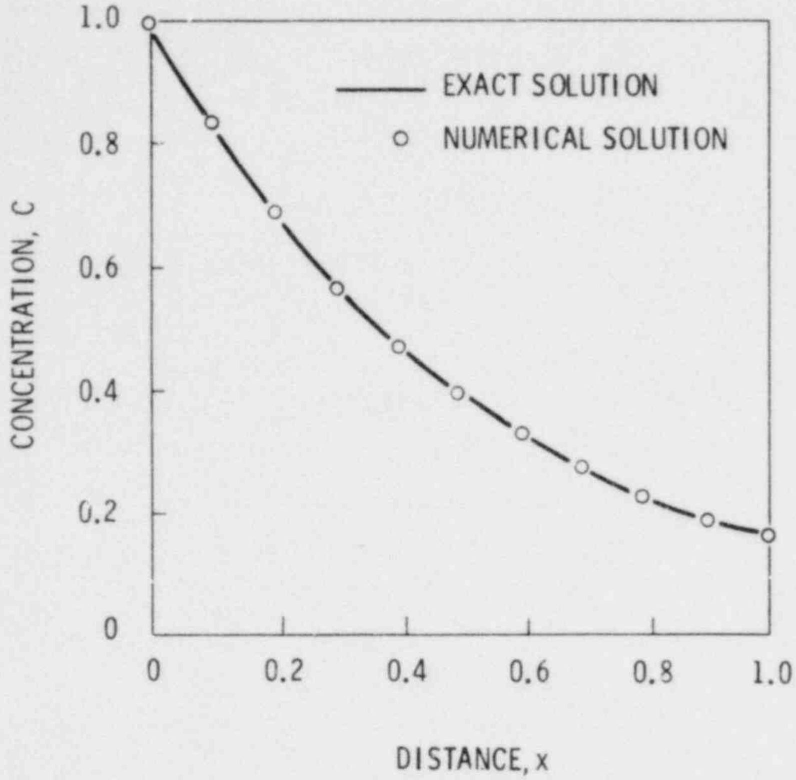

FIGURE 2. Comparison of Numerical Solution with Analytical Solution of One-Dimensional Steady Convection-Diffusion Equation with a Decay Term

Example 2

In this second example, convergence of a time-dependent, one-dimensioal solution to a steady-state solution was tested. The governing equation was:

$$\frac{\partial C}{\partial t} = \varepsilon_x \frac{\partial^2 C}{\partial x^2} - \alpha C$$

with the following boundary condition:

$C = 0$	in $0 \leq x \leq \ell$	at	$t = 0$
$C = C_o$	at $x = 0$	at	$t > 0$
$\frac{\partial C}{\partial t} = 0$	at $x = \ell$	for all	t

Assuming $\varepsilon_x = 0.2$, $\alpha = 1.0$, $C_o = 1.0$ and $\ell = 1.0$, solutions are plotted in Figure 3, together with steady analytical and numerical solutions of the following equation:

$$\varepsilon_x \frac{\partial^2 C}{\partial x^2} - \alpha C = 0$$

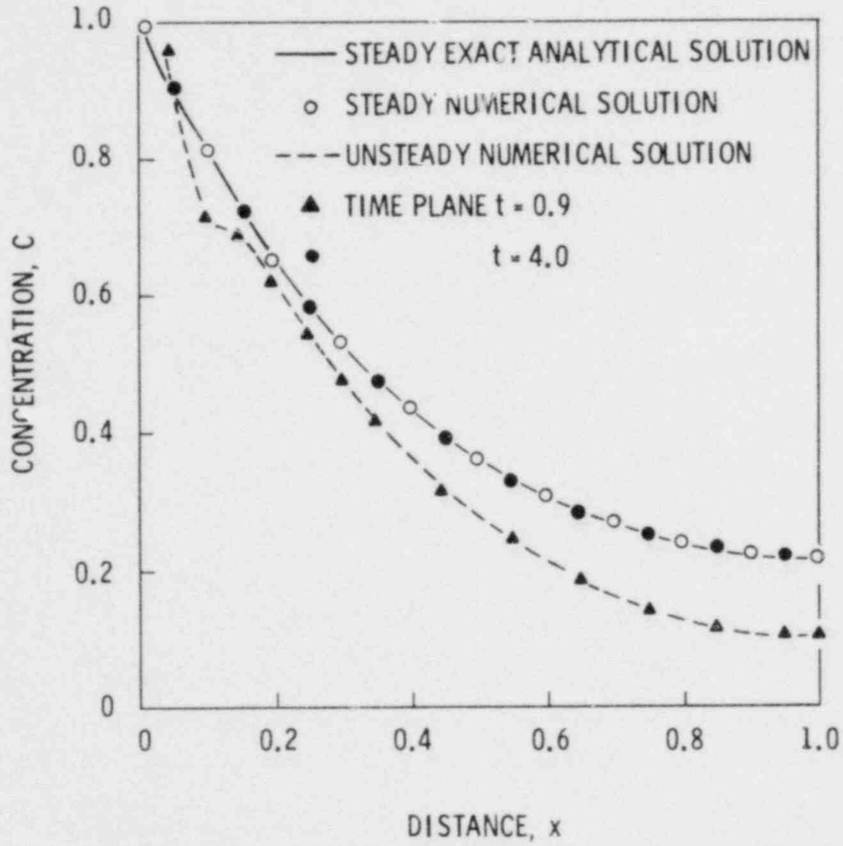

FIGURE 3. Convergence of Unsteady-State One-Dimensional Diffusion Equation to Steady-State Solution

As shown in Figure 3, unsteady numerical solutions converged to the steady-state exact solution. For runs with time t greater than 4.0, the numerical solutions coincide with the steady state analytical solution. The steady-state numerical solution also agrees well with the exact solution.

Example 3

The following two-dimensional equation was solved numerically and computed results were compared with an analytical solution:

$$\varepsilon_x \frac{\partial^2 C}{\partial x^2} + \varepsilon_y \frac{\partial^2 C}{\partial y^2} = 0$$

with boundary conditions of:

$C = 0$	at	$x = 0$
$C = 0$	at	$x = \ell$
$C = 0$	at	$y = 0$
$C = C_o \sin\left(\frac{\pi x}{\ell}\right)$	at	$y = \ell$

where $\varepsilon_x = \varepsilon_y = \ell = 1.0$ and $C_o = 10$. The analytical solution for this case is:

$$C(x,y) = 0.866 \sinh(\pi y) \sin(\pi x)$$

The computer results and analytical solutions are shown in Figure 4. Numbers in the figure are values of concentration C. Since the solutions are symmetric with respect to $x = 0.5$, computer results are given in the region of $0.5 \leq x \leq 1.0$, and analytical solutions are plotted in the region of $0 \leq x < 0.5$. Comparison of these results reveals that there is an excellent agreement between the computed and analytical solutions.

As illustrated in Figures 2 through 4 the agreements of the model solutions and the exact solutions were excellent. Further validation of the basic computational scheme of FETRA with both linear and quadratic approximations to velocity and depth distributions are currently underway.

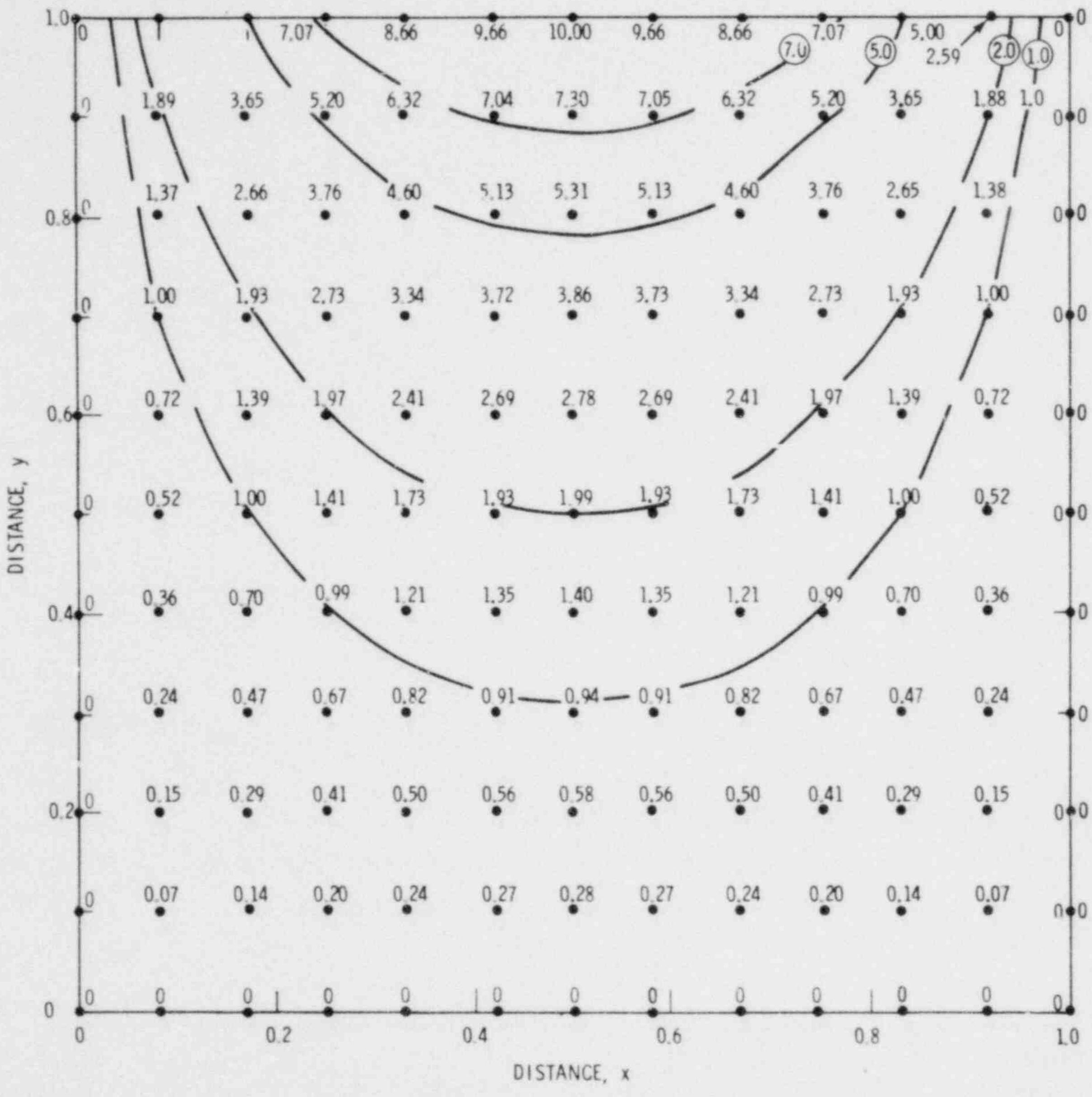

FIGURE 4. Comparison of Numerical Solution with Analytical Solution to Two-Dimensional Diffusion Equation

4. SOME COMPUTATIONS OF SEDIMENT TRANSPORT CAPACITY UNDER MARINE ENVIRONMENT

The primary modification made to FETRA was to include the wave-sediment interaction which occur in marine and large lacustrine environment. In this chapter, sediment transport capacity, Q_T in Equations (28) and (35) for offshore and surf zones were calculated. These values would then be used to calculate noncohesive sediment erosion and deposition rate, S_{Rj} and S_{Pj}, by Equations (14) and (15).

First, noncohesive sediment transport capacities in an offshore zone were calculated by FETRA under six different wind conditions. Calculated results of characteristics of waves induced by wind and the resulting sediment transport capacities are shown in Table 1, together with input data. Input data for these six runs were identical except for the wind velocity which was increased from 25 knots to 50 knots in increments of 5 knots. Although there are no data to be compared, the computed sediment loads follow the expected trend, i.e., a higher wind velocity results in a greater sediment transport rate. The table also indicates that the ratio of suspended load to the total load increases from 0.20 to 0.75, as the wind speed increases from 25 knots to 50 knots.

The noncohesive sediment transport capacity in a surf zone was also computed by FETRA. Assumed input data and predicted sediment load are presented in Table 2. The computed littoral transport rate was compared with the value reported in the U.S. Corps of Engineers Shore Protection Manual (1973), as shown in Figure 5. Solid lines in Figure 5 are those reported in the Shore Protection Manual. Comparison of these two cases indicates that FETRA predicted littoral transport rate to be 3.39 x 10^7 kg_f/day, while the Shore Protection Manual indicates 4.05 x 10^7 kg_f/day. Hence FETRA's value is approximately 20% smaller. The Shore Protection Manual reports that the empirical formula used in the Manual tends to overestimate the sediment transport capacity at higher values of wave breaking height and breaker angle. The same report also states that the formula used in the Shore

TABLE 1. Computed Wave Characteristics and Sediment Transport Capacity Under Marine Environment

Identification	Depth, m	Fetch Length, m	Wind Velocity, knots	External Current, m/sec	Viscosity, m2/sec	Sediment Diameter, mm	Sediment Density kgf-sec2/m4	Water Density kfg-sec2/m4	Wave Number, m	Wave Amplitude, m	Wave Frequency sec	Bed Load, kgf/day-m	Suspended Load, kgf/day-m	Total Load kgf/day-m
1	7.5	80,000	25	0	9.76×10^{-7}	65	288.66	102.	0.2187	0.4332	1.410	0.19	0.05	0.24
2	7.5	80,000	30	0	9.76×10^{-7}	65	288.66	102.	0.1930	0.4930	1.301	0.66	0.39	1.05
3	7.5	80,000	35	0	9.26×10^{-7}	65	288.66	102.	0.1752	0.5455	1.219	1.14	1.22	2.36
4	7.5	80,000	40	0	9.76×10^{-7}	65	288.66	102.	0.1621	0.5925	1.154	1.60	2.66	4.26
5	7.5	80,000	45	0	9.76×10^{-7}	65	288.66	102.	0.1519	0.6352	1.101	2.07	4.79	6.86
6	7.5	80,000	50	0	9.76×10^{-7}	65	288.66	102	0.14[illegible]7	0.6745	1.057	2.56	7.8	10.24

TABLE 2. Input Parameters and Computed Sediment Transport Capacity in a Surf Zone

Input	Data	Computer Sediment Load	
Depth	1.561 m	Surf Zone Littoral Transport	3.39×10^7 kg_f/day
Wave Height at Breaking	1.[illegible]19 m		
Wave Number	0.321 m^{-1}		
Sediment De[illegible]y	188.6 kg_f-sec^2/m^4		
Water Density	102.0 kg_f-sec^2/m^4		
Breaker Angle with Shoreline	45°		

Protection Manual estimates approximately tw[illegible]ce the equivalent val[illegible] from the design curve (Figure 2-22) of the U.S. Army Coastal Engineering Research Center (CERC) technical Report No. 4 (1966). Hence the predicted noncohesive sediment transport capacity in a surf zone computed by FETRA is reasonable.

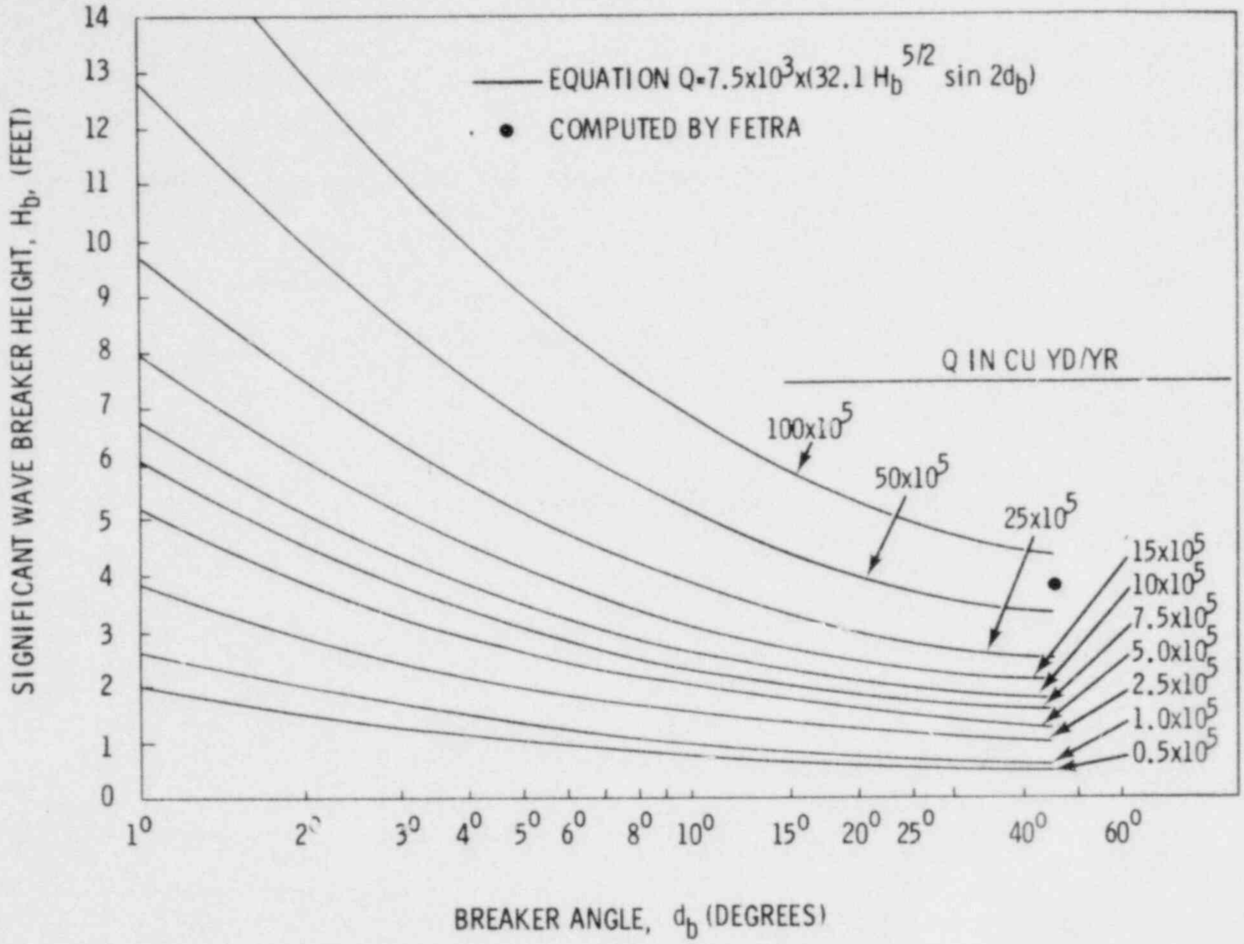

FIGURE 5. Longshore Transport Rate as a Function of Breaker Height and Breaker Angle, Together with Sediment Load Computed by the FETRA Code

REFERENCES

Bretscheider, C. L. and R. O. Reid. 1953. "Change in Wave Height Due to Bottom Friction, Percolation and Refraction," 34th Annual Meeting of American Geophysics Union.

Churchill, M. A., J. A. Cragwall, Jr., R. W. Andres, and S. L. Jones. 1965. Concentrations, Total Stream Loads, and Mass Transport of Radionuclides in the Clinch and Tennessee Rivers. ORNL-3721, Suppl. I, Oak Ridge National Laboratory, Oak Ridge, TN.

Dobson, R. S. 967. Some Applications of a Digital Computer to Hydraulic Engineering Problems. Technical Report No. 80, Stanford University, Department of Civil Engineering.

Ecker, R. M. and H. [illegible] 1974. "Sediment Transport Coast of Northern California." ASCE N[illegible]ing on Water Resources Engineering, January 21-25, Los An[illegible]A.

Einstein, H. A. 1972. "Sediment Transport by Wave Action." Proceedings of 13th Conference on Coastal Engineering, ASCE.

Hetherington, J. A. 1975. "The Behavior of Plutonium Nuclides in the Irish Sea," Environmental Toxicity of Aquatic Radionuclides: Models and Mechanisms. M. W. Miller and J. N. Stannard (editors), Ann Arbor Science Publishers, Ann Arbor, MI.

Hauschild, W. L., R. W. Perkins, H. H. Stevens, G. R. Dempster, Jr., and J. L. Glenn. 1966. "Progress Report--Radionuclide Transport of the Columbia River, Pasco to Vancouver, Washington Reach, July 1962 to September 1963," Open-file report, U.S. Geological Survey, Portland OR.

Komar, P. D. 1977. "Modeling of Sand Transport on Beaches and the Resulting Shoreline Evolution." The Sea. Vol. 6, John Wiley and Sons, pp. 499-513.

Krone, R. B. 1962. Flume Studies of the Transport of Sediment in Estuarial Shoaling Processes, Hydraulic Engineering Laboratory and Sanitary Engineering Research Laboratory, University of California at Berkeley.

Leendertse, J. J. 1970. "A Water Quality Simulation Model for Well Mixed Estuaries and Coastal Seas, Principles of Computation, Volume I," RM-6230-RC, The Rand Corp., Santa Monica, CA.

Liang, S. S. and Wang, H. 1973. Sediment Transport in Random Waves. Technical Report No. 26, University of Delaware, College of Marine Studies.

Norton, W. R., L. A. Roesner, D. E. Evenson and J. R. Monser. 1974. "Computer Program Documentation for the Stream Quality Model, QUAL-II," Water Resources Engineers, Inc., Walnut Creek, CA.

Oak Ridge National Laboratory. 1977. Proceedings of the Workshop on the Evaluation of Models Used for the Environmental Assessment of Radionuclide Releases. CONF-770901, Gatlinburg, TN.

Onishi, Y., P. A. Johanson, R. G. Baca, and E. L. Hilty. 1976. Studies of Columbia River Water Quality--Development of Mathematical Models for Sediment and Radionuclide Transport Analysis. BNWL-B-452, Battelle, Pacific Northwest Laboratories, Richland, WA.

Onishi, Y. 1977. Mathematical Simulation of Sediment and Radionuclide Transport in the Columbia River. BNWL-2228, Battelle, Pacific Northwest Laboratories, Richland, WA.

Onishi, Y. and S. E. Wise. 1978. "Mathematical Modeling of Sediment and Contaminant Transport in the James River Estuary," Proceedings of 27th Annual Hydraulic Division Speciality Conference of ASCE. College Park, Ma, pp. 303-310.

Onishi, Y. E. M. Arnold, R. J. Serne, C. E. Conway, F. L. Thompson, and D. W. Mayer. 1979a. "Annual Report--October 1977 to September 1978--Mathematical Simulation of Sediment and Contaminant Transport in Surface Waters," NUREG/CR-0658, PNL-2902, Pacific Northwest Laboratory, Richland, WA.

Onishi, Y. 1979. "Evaluation of Mathematical Models of Hazardous Substances on Surface Waters," Proceedings of U.S. Environmental Protection Agency's, "National Workshop of Verification of Water Quality Models," West Point, NY.

Onishi, Y., D. L. Schreiber, and R. B. Codell. 1979b. "Mathematical Simulation of Sediment and Radionuclide Transport in the Clinch River, Tennessee," Proceedings of ACS/CSJ Chemical Congress, Honolulu, Hawaii, April 2-7, 1979, "Processes Involving Contaminants and Sediment," edited by R. A. Baker, Ann Arbor Publisher, Inc.

Onishi, Y. and S. E. Wise. 1979c. "Finite Element Model for Sediment and Toxic Contaminant Transport in Streams," Proceedings of Hydraulic and Energy Divisions Speciality Conference of ASCE on "Conservation and Utilization of Water and Energy Resources," San Francisco, CA, pp. 144-150.

Onishi, Y., S. M. Brown, A. R. Olsen, M. A. Parkhurst, S. E. Wise and W. H. Walters. 1979d. "Methodology for Overland and Instream Migration and Risk Assessment of Pesticides." Submitted to U.S. Environmental Protection Agency by Battelle, Pacific Northwest Laboratories, Richland, WA.

Pagenkopf, J. R., G. C. Christodoulou, B. R. Pearce an J. J. Connor. 1976. A User's Manual for "CAFE-1", A Two-Dimensional Finite Element Circulation Model. Report No. 217, Massachusetts Institute of Technology, Department of Civil Engineering.

Partheniades, E. 1962. A Study of Erosion and Deposition of Cohesive Soils in Salt Water, Ph.D. Thesis, University of California at Berkeley.

Schlichting, H. 1968. Boundary-Layer Theory. McGraw Hill Book Co.

Sverdrup, H. U. and W. H. Munk. 1947. "Wind, Sea and Swell; Theory of Relationships for Forecasting," Pub. No. 601, U.S. Navy Hydrographic Office, Washington, DC.

U.S. Army Corps of Engineers, Beach Erosion Board. 1962. "Waves in Inland Reservoirs, Summary Report on Civil Works Investigation Projects CW-164 and CW-165," Tech. Memo No. 132.

U.S. Army Corps of Engineers. Coastal Engineering Research Center. 1966. "Shore Protection, Planning and Design," Technical Report No. 4, Third Edition.

U.S. Army Corps of Engineers, Coastal Engineering Research Center. 1973. "Shore Protection Manual," Vol. 3.

U.S. Environmental Protection Agency. 1978. "Kepone Mitigation Project Report," Standard and Criteria Office of Water and Hazardous Materials, Washington, DC.

U.S. Nuclear Regulatory Commission. 1973. Regulatory Guide 1.113--Estimating Aquatic Dispersion of Effluents from Accidental and Routine Reactor Releases for the Purpose of Implementing, Appendix I.

U.S. Nuclear Regulatory Commission. 1978. "Liquid Pathway Generic Study--Impacts of Accidental Radioactive Releases to the Hydrosphere for Floating and Land-Based Nuclear Power Plants," NUREG-0440, Washington, DC.

Vanoni, V. A. 1975. Sedimentation Engineering. Prepared by the ASCE Task Committee for the Preparation of the Manual on Sedimentation of the Sedimentation Committee of the Hydraulics Division, New York, NY.

NUREG/CR-1026
PNL-3114
RE

DISTRIBUTION LIST

No. of Copies

OFFSITE

A. A. Churm
DOE Patent Division
9800 South Case Avenue
Argonne, IL 60439

200 U.S. Nuclear Regulatory Commission
Division of Technical Information and Document Control
7920 Norfolk Avenue
Bethesda, MD 20014

2 DOE Technical Information Center

C. V. Alonso
U.S. Department of Agriculture
Sedimentation Laboratory
Southern Region
Agricultural Research Center
P.O. Box 1157
Oxford, MI 38655

R. A. Baker
U.S. Geological Survey
National Space Technology Laboratories
NSTL Station, MS 39529

J. J. Cassidy, Director
Water Research Center
Washington State University
Pullman, WA 99164

H. B. Fisher
Department of Civil Engineering
University of California at Berkeley
Berkeley, CA 94720

No. of Copies

E. F. Gloyna
College of Engineering
University of Texas at Austin
Austin, TX 78705

F. O. Hoffman
Oak Ridge National Laboratory
Oak Ridge, TN 37830

E. R. Holley
Department of Civil Engineering
University of Illinois
Urbana, Illinois 61801

Irving Joseph
Bechtel Corporation
50 Beale Street
San Francisco, CA 94105

G. H. Jirka
Department of Environmental Engineering
Cornell University
Ithaca, NY 14850

J. F. Kennedy
Institute of Hydraulic Research
University of Iowa
Iowa City, Iowa 52241

R. B. Krone
Department of Civil Engineering
University of California at Davis
Davis, CA 95616

No. of Copies		No. of Copies	

E. Partheniades
Department of Engineering Science
University of Florida
Gainesville, Florida 32611

Dr. P. J. Ryan
Bechtel Corporation
50 Beale Street
San Francisco, CA 94105

H. G. Stefan
Department of Divil and Mineral Engineering
University of Minnesota
Minneapolis, MN 55455

J. Steger
Health Division
Mail Stop 490
Los Alamos Scientific Laboratory
P.O. Box 1663
Los Alamos, NM 87545

W. J. Garrett
Corps of Engineers
New Orleans District
P.O. Box 60261
New Orleans, LA 70160

W. McAnally
Corps of Engineers
U.S. Army Engineering Waterways Experiment Station
Vicksburg, MS 39180

W. A. Thomas
Corps of Engineers
U.S. Army Engineering Waterways Experiment Station
Vicksburg, MS 39180

B. R. Winkley
Corps of Engineers
Vicksburg District
Vicksburg, MS 39180

C. A. Little
Health and Safety Research Division
Oak Ridge National Laboratory
P.O. Box X
Oak Ridge, TN 37830

R. B. Ambrose
Environmental Protection Agency
Environmental Research Laboratory
Athens, GA 30603

J. W. Falco
Environmental Protection Agency
Environmental Research Laboratory
Athens, GA 30603

L. A. Mulkey
Environmental Protection Agency
Environmental Research Laboratory
Athens, GA 30603

M. Shirazi
Environmental Protection Agency
Pacific Northwest Water Laboratory
200 S.W. 35th Street
Corvallis, OR 97331

P. Datta
Environmental Protection Agency
Office of Pesticide Program
Washington, DC 20460

W. L. Richardson
Environmental Protection Agency
Large Lakes Research Station
9311 Groh Road
Grosse Isle, MI 48138

P. C. Benedict
U.S. Geological Survey
345 Middlefield Road
Menlo Park, CA 21201

No. of
Copies

L. E. Young
Water Resources Division
U.S. Geological Survey
345 Middlefield Road
Menlo Park, CA 94025

N. Yotsukura
U.S. Geological Survey
Water Resources Division
National Center
12201 Sunrise Valley Dr.
Reston, VA 22092

W. Bevins
U.S. Nuclear Regulatory Commission
Washington, DC 20555

R. B. Codell
U.S. Nuclear Regulatory Commission
Washington, DC 20555

No. of
Copies

P. R. Reed
U.S. Nuclear Regulatory Commission
Washington, DC 20555

F. Swanberg
U.S. Nuclear Regulatory Commission
Washington, DC 20555

ONSITE

14 Pacific Northwest Laboratory

E. M. Arnold
D. B. Cearlock
D. W. Dragnich
D. W. Mayer
Y. Onishi (2)
Technical Information (5)
Publishing Coordination RO (2)
Water and Land Resources Library